Journal of Crystal Growth 333 (2011) 16–19

Contents lists available at SciVerse ScienceDirect

Journal of Crystal Growth

journal homepage: www.elsevier.com/locate/jcrysgro

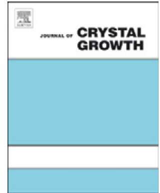

Hydrogen etching of GaN and its application to produce free-standing GaN thick films

Yen-Hsien Yeh *, Kuei-Ming Chen, Yin-Hao Wu, Ying-Chia Hsu, Tzu-Yi Yu, Wei-I Lee

Department of Electrophysics, National Chiao Tung University, Hsinchu 30010, Taiwan

ARTICLE INFO

Article history:
Received 2 May 2011
Received in revised form
15 July 2011
Accepted 16 August 2011
Communicated by R. Bhat
Available online 23 August 2011

Keywords:
A1. Hydrogen etching
A1. Surface processes
A1. Surface structure
A3. Hydride vapor phase epitaxy
B1. Nitrides
B2. Semiconducting III–V materials

ABSTRACT

This work investigates the morphology of GaN etched in hydrogen (H_2) at different temperatures, the activation energies of the rate-limiting steps of H_2 etching, and the overgrowth on a H_2-etched GaN template. The surfaces of GaN have different profiles after being etched in H_2; they resemble a plane decorated with columns and mooring posts in a low-temperature etching condition, and with deep cavities in a high-temperature etching condition. The etched profiles show that H_2 etching has controllable etching directions: vertical and lateral. In a low-temperature condition, H_2 etching has both vertical and lateral etching directions; however, in a high-temperature condition, it has only the vertical etching direction. The activation energies of the rate-limiting steps under etching pressures of 100 and 700 Torr are estimated to be 3.22 and 3.77 eV, respectively. A thick GaN layer has been grown on a H_2-etched GaN template, and it has self-separated from the underlying sapphire substrate.

© 2011 Elsevier B.V. All rights reserved.

1. Introduction

GaN is a major wide band gap semiconductor used in fabricating green to ultraviolet optoelectronic devices. Various processes have been developed to study the properties of GaN; among them, etching is one of the most important steps. For example, the etching process is necessary for making a patterned structure on the surface of GaN to reduce stress and dislocation density during the manufacturing of devices or large-area free-standing GaN substrates [1–5]. Unfortunately, conventional wet etching is difficult to be used due to the high chemical stability of GaN. The more effective methods are dry etching techniques such as reactive ion etching (RIE) [6] and inductively coupled plasma (ICP) [7]. These dry etching processes produce anisotropic etching, i.e., GaN is etched in the vertical direction. However, the obtainable patterned structures are limited because of the single direction etching. It is valuable to develop an etching technique having both vertical and lateral etching directions. Additionally, an in situ maskless etching will also help to simplify the manufacturing processes of GaN substrates and devices.

In our previous work, the morphology of GaN etched in hydrogen (H_2) under different pressures had been studied [8]. A model was developed to explain the mechanism of H_2 etching under different pressures at 1050 °C. We found that H_2 etching begins at some weak areas such as dislocation sites, and all vicinity of dislocation sites has been etched to form cavities. In this work, we investigate the morphology of GaN etched in H_2 at different temperatures, the activation energies of the rate-limiting steps of H_2 etching, and the overgrowth on a H_2-etched GaN template.

2. Experiment

Samples used in the experiments were MOCVD-grown *c*-plane GaN template layers on sapphire, and the thickness of the GaN layers was about 2 μm. The first experiment was temperature-varying etching. After ultrasonic cleaning, a sample was loaded into a home-made horizontal HVPE reactor, and then the reactor was heated to a desired temperature under a pressure of 700 Torr. In addition to nitrogen (N_2), ammonia (NH_3) was also introduced into the reactor to avoid GaN decomposition during heating. After the temperature reached, NH_3 was shut off, and H_2 was introduced to begin etching. The flow rates of H_2 and N_2 were 1 and 4.9 slm, respectively; the etching time was 10 min. Six samples labeled A, B, C, D, E, and F were etched at the temperatures of 1050, 1060, 1070, 1080, 1090, and 1100 °C, respectively. The surface morphologies of the etched samples were observed through a high-resolution field emission scanning electron microscope (FE-SEM, Hitachi s-4700i). The second experiment is the calculation of the activation energy of the reaction limiting GaN decomposition. Samples were weighed to within 0.1 mg using an

* Corresponding author.
E-mail address: a8550106@ms19.hinet.net (Y.-H. Yeh).

0022-0248/$ - see front matter © 2011 Elsevier B.V. All rights reserved.
doi:10.1016/j.jcrysgro.2011.08.022

analytical balance before etching, and then they performed H_2 etching at different temperatures by HVPE. After H_2 etching, each sample was reweighed to determine the mass loss. The etching rate was calculated from the mass loss divided by the etching area and time. Two activation energies at etching pressures of 100 and 700 Torr have been estimated. The third experiment was the overgrowth on a H_2 etched sample by HVPE. The H_2-etching condition was a two-step etching that was described in our previous study [8]. After etching, a 320 μm-thick GaN layer was sequentially grown on the sample at 1050 °C under the high pressure of 700 Torr for 120 min, and the V/III ratio was 40.

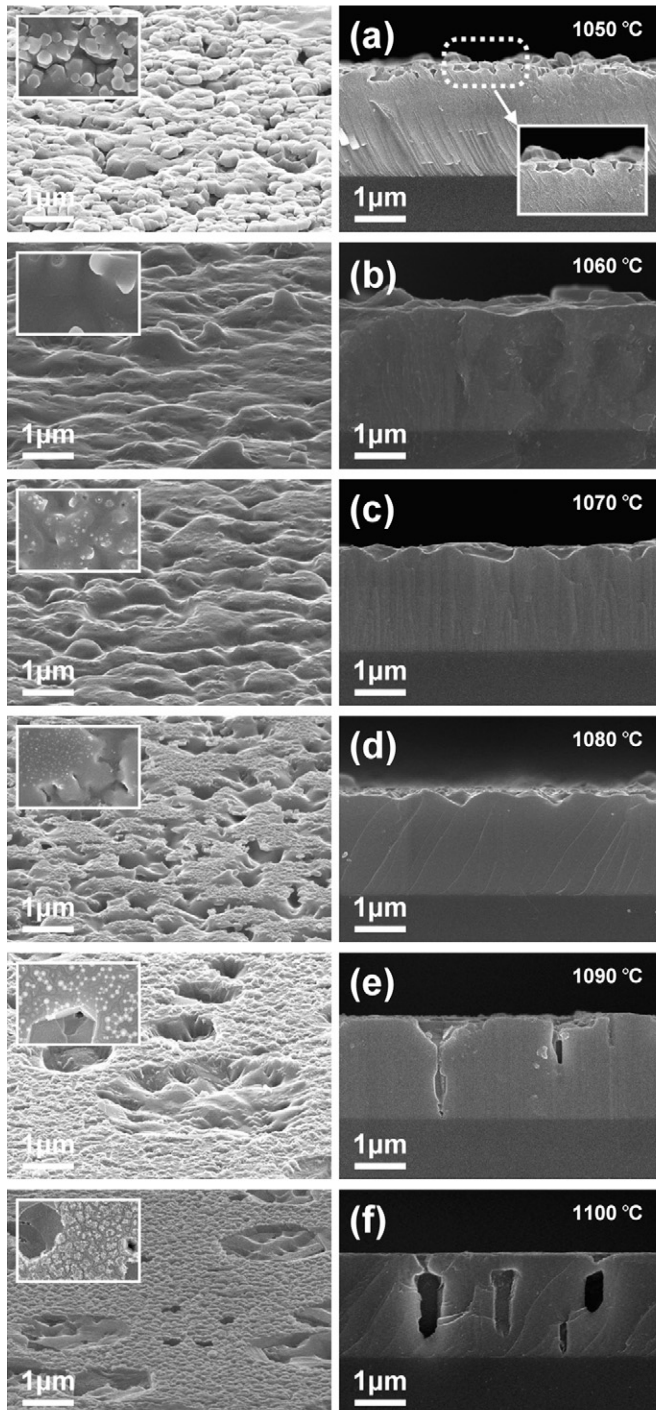

Fig. 1. SEM images of the samples etched at different temperatures in plan views (insets), tilted views (left column) and cross-section views (right column): (a) 1050, (b) 1060, (c) 1070, (d) 1080, (e) 1090, and (f) 1100 °C. All the scale bars are 1 μm.

3. Result and discussion

Fig. 1 shows SEM images of the six samples etched at the temperatures of 1050–1100 °C. It can be found that the etching temperature has remarkable influence on the morphologies of GaN surfaces. The surface resembles a plane decorated with mooring posts or columns at the low etching temperature of 1050 °C, as shown in Fig. 1(a), and there are a lot of undercut shapes revealing the lateral etching ability of H_2 etching. As a higher etching temperature is used, the surface becomes flatter. Deep cavities begin to appear at the high temperature of 1090 °C, and the density of them becomes larger at the highest temperature of 1100 °C.

We can compare the effects of temperature with those of pressure. By comparing our previous study [8], it can be found that the effects of temperature are similar to those of pressure but with an opposite tendency, i.e., in the pressure-varying experiment, the etched surfaces are decorated with bollard-like posts at high pressures and with deep cavities at low pressures.

The mechanism of the formation of the morphologies at these temperatures can be explained by a model, which is similar to the one we proposed in our previous study. It has been reported that H_2 enhances GaN decomposition; H and N atoms combine to form NH_3 [9–13]. As H mostly reacts with N, we presume that during H_2 etching, a facet formed with N atoms (N-terminated) will be unstable whereas a facet formed with Ga atoms (Ga-terminated) will be stable. The as-grown surface of a MOCVD-grown *c*-plane GaN film is Ga-polarity (Ga-face) and the reverse side is N-polarity (N-face); the inclined {10–11}, {11–22} facets are mainly N-terminated; however, the nonpolar (*a*-plane and *m*-plane) facets contain equal number of Ga and N atoms. Therefore, we suppose that during H_2 etching, the relative stabilities of the facets follow the order: Ga-face > nonpolar face > inclined face > N-face. At 1050 °C under 700 Torr, the etching mechanism is proposed to be as follows. As H_2 arrives at the surface, it is difficult to decompose most of GaN on the surface due to the high stability of Ga-polarity. Thus, etching occurs at some weak areas such as dislocation sites to form a vertical cavity, as shown in Fig. 2(b) (the dotted line indicates a dislocation). As H_2 etch GaN downwardly, the products, NH_3 and N_2,

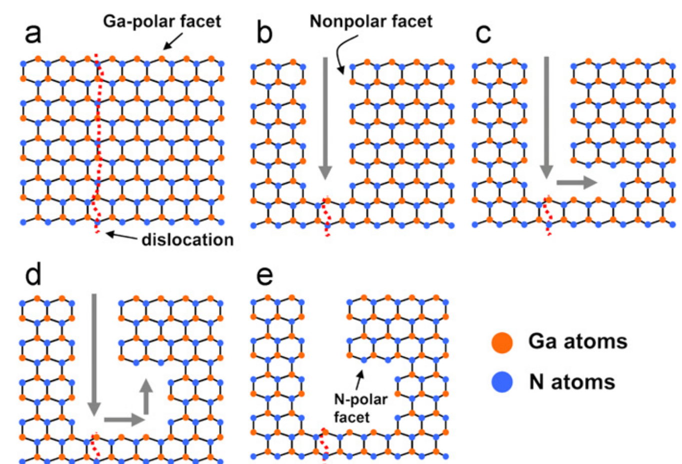

Fig. 2. Stages of H_2 etching at low temperature: (a) unetched template, the top surface is Ga-face and the dotted line indicates the dislocation, (b) H_2 etching at the dislocation site, (c) lateral etching at the bottom of the cavity, and then N-face facet is exposed, (d) etching in the upward direction due to the instability of N-face, and (e) the resulting etching profile.

are produced; they dissipate slowly and then occupy the bottom of the cavity at the low temperature of 1050 °C under 700 Torr. H_2 cannot flow into the bottom of the cavity due to the occupancy of NH_3 and N_2; therefore, the bottom of the cavity becomes a high V/III ratio environment. It is proposed from the previous researches that the inclined faces are stable in a condition of high V/III ratio [3,5,14]. Hence, we infer that the nonpolar sidewalls become unstable in such an environment. As a result, the lateral etching begins at the bottom of the cavity, as shown in Fig. 2(c). After the sidewalls are etched for some distance, the N-face facet is exposed, and then it is etched due to its instability; therefore, etching begins in the upward direction, as shown in Fig. 2(d). The resulting etching profile is shown in Fig. 2(e), and it has an undercut shape. A lot of cavities with this undercut profile expand and merge to make the morphology resemble a surface decorated with columns or mooring posts, as shown in Fig. 1(a).

The formation of the cavities at a low etching pressure in our previous study is proposed as follows. As the pressure become lower, NH_3 and N_2 dissipate more rapidly, and the bottom of the cavity becomes a H_2 environment; the sidewalls become stable, and deep cavities appear. We suggest the formation of the cavities at high etching temperatures is also due to a similar mechanism. At high temperature, the dissipation rate of NH_3 and N_2 increases, so the bottom of the cavity becomes a H_2 environment; therefore, the sidewalls become stable, and deep cavities appear as a result.

To estimate the activation energies of the rate-limiting steps of H_2 etching under pressures of 100 and 700 Torr, we performed experiments to obtain the etching rates at different temperatures. Fig. 3 shows the Arrhenius plot of the results, and we estimate the activation energies at the etching pressures of 100 and 700 Torr to be about 3.22 and 3.77 eV, and the pre-exponential factors of them are 3.34×10^{27} and 2.62×10^{29} molecules/cm^2 s, respectively. These values indicate that the rate-limiting steps for H_2 etching at 1030–1055 °C under pressures of 100 and 700 Torr are the same, i.e., formation and the desorption of N_2 [9]. However, the different activation energies may have some implications. In Ref. [9], the activation energy of the etching condition under pure H_2 at 40 and 76 Torr is 3.4 eV, and that under pure N_2 at 76 and 150 Torr is 3.62 eV; the activation energy under pure N_2 is larger. In our results, the activation energy under the high pressure of 700 Torr is larger than that of 100 Torr (the same H_2/N_2 ratio), so we infer this result agrees with our hypothetical model that the bottom of the cavities is relatively a high V/III ration environment (without H_2) at high pressure and a H_2 environment at low pressure [8]. The sidewalls are unstable at high pressure, and then the lateral etching begins as the mechanism discussed in Ref. [8].

To demonstrate the application of H_2 etching, we performed an overgrowth experiment. A sample was first etched using two-step etching to produce porous caves structure that is shown in

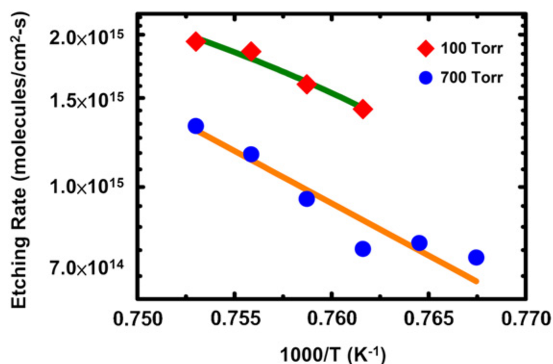

Fig. 3. The Arrhenius plot of the etching rates at pressures of 100 and 700 Torr.

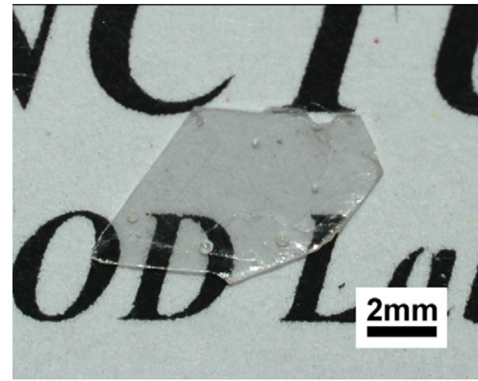

Fig. 4. The free-standing GaN thick film.

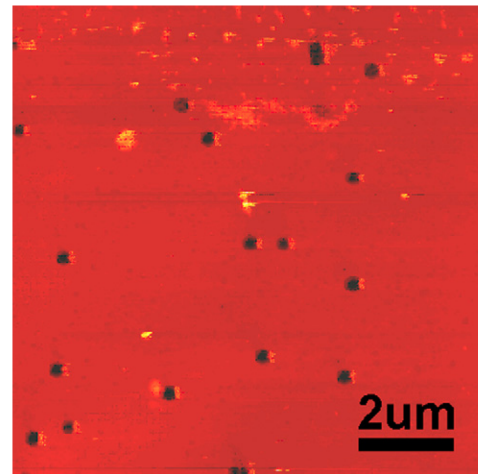

Fig. 5. AFM image of the self-separated sample after an EDP experiment.

our previous study [8], and then a 320 μm-thick GaN layer was grown on the sample. The overgrown GaN thick layer self-separated from the underlying sapphire substrate; however, it also cracked. The growth area is 10 mm × 10 mm, and the largest piece is shown in Fig. 4. It is supposed that the porous caves make the interface of the GaN layer and the sapphire substrate become weak, so the thick film separates from the substrate due to the stress that rises during cooling. Nevertheless, the etching and growth parameters need to be optimized to avoid cracks. This experiment demonstrates one possible application of H_2 etching, and we believe that H_2 etching is also helpful for the reduction of threading dislocation density during the overgrowth process; however, the dislocation density of the self-separated sample does not reduce greatly. Fig. 5 shows the AFM image of the surface of the free-standing GaN thick film after an EDP experiment. The dislocation density is estimated to be about 2×10^7 cm^{-2}, and this value is just a little lower than that of a thick film, which is grown without H_2 etching. We consider that the growth condition needs to be optimized to reduce the dislocation density.

4. Summary

In conclusion, different morphologies appear on the GaN surface etched in H_2 at different temperatures under a high pressure of 700 Torr. It is considered that H_2 etching begins in certain weak areas such as dislocation sites. In addition to the vertical downward direction, H_2 etching also has lateral and

upward directions at the low temperature of 1050 °C, and these etching directions make the surface profile resemble a plane clustered with columns or mooring posts. On the other hand, H_2 etching merely has the vertical direction at high temperatures that make the surface decorate with cavities. The activation energies of the rate-limiting steps at pressures of 100 and 700 Torr are estimated to be 3.22 and 3.77 eV, respectively. A 320 μm-thick GaN layer has been grown on a H_2-etched GaN template, and it has self-separated from the underlying sapphire substrate.

Acknowledgment

This work was financially supported by National Science Council of Taiwan (Contract no. NSC 98-2221-E-009–026).

References

[1] A. Sakai, H. Sunakawa, A. Usui, Applied Physics Letters 71 (1997) 2259.
[2] O.-H. Nam, M.D. Bremser, T.S. Zheleva, R.F. Davis, Applied Physics Letters 71 (1997) 2638.
[3] K. Hiramatsu, K. Nishiyama, A. Motogaito, H. Miyake, Y. Iyechika, T. Maeda, Physica Status Solidi A 176 (1999) 535.
[4] I. Kidoguchi, A. lshibashi, G. Sugahara, Y. Ban, Applied Physics Letters 76 (2000) 3768.
[5] K. Hiramatsu, K. Nishiyama, M. Onishi, H. Mizutani, M. Narukawa, A. Motogaito, H. Miyake, Y. Iyechika, T. Maeda, Journal of Crystal Growth 221 (2000) 316.
[6] M.E. Lin, Z.F. Fan, Z. Ma, L.H. Allen, H. Morkoç, Applied Physics Letters 64 (1994) 887.
[7] R.J. Shul, G.B. McClellan, S.A. Casalnuovo, D.J. Rieger, S.J. Pearton, C. Constantine, C. Barratt, Applied Physics Letters 69 (1996) 1119.
[8] Y.H. Yeh, K.M. Chen, Y.H. Wu, Y.C. Hsu, W.I. Lee, Journal of Crystal Growth 314 (2011) 9.
[9] D.D. Koleske, A.E. Wickenden, R.L. Henry, J.C. Culbertson, M.E. Twigg, Journal of Crystal Growth 223 (2001) 466.
[10] T.H. Myers, B.L. VanMil, J.J. Holbert, C.Y. Peng, C.D. Stinespring, J. Alam, J.A. Freitas Jr., V.A. Dmitriev, A. Pechnikov, Y. Shapovalova, V. Ivantsov, Journal of Crystal Growth 246 (2002) 244.
[11] N. Kobayahi, Y. Kobayahi, Applied Surface Science 159–160 (2000) 398.
[12] M.A. Mastro, O.M. Kryliouk, M.D. Reed, T.J. Anderson, A.J. Shapiro, Physica Status Solidi A 188 (2001) 467.
[13] M. Mayumi, F. Satoh, Y. Kumagai, K. Takemoto, A. Koukito, Japanese Journal of Applied Physics 39 (Part 2) (2000) L707.
[14] Hai-Ping Liua, Jenq-Dar Tsayb, Wen-Yueh Liub, Yih-Der Guob, Jung Tsung Hsub, In-Gann Chen, Journal of Crystal Growth 260 (2004) 79.